Inter- and Intramolecular Stacking Interaction between Indole and Adeninium Rings†

Toshimasa Ishida,* Megumi Shibata, Kaho Fujii, and Masatoshi Inoue

ABSTRACT: Crystals of 1,9-dimethyladeninium–indole-3-acetate (1:1) complex (I) and 9-(3-indol-3-ylpropyl)-1-methyladeninium iodide (II), an inter- or intramolecular model for the stacking interaction between the tryptophanyl residue and the methylated (or protonated) adenine base, were subjected to X-ray analyses. Nearly parallel stacking and interplanar spacing near to 3.4 Å were observed between the indole and adeninium rings of both crystals. In particular, one of the two stacking pairs formed in I showed the existence of a partial charge-transfer interaction in their ground states. On the basis of the molecular orbital consideration, the mutual orientation between these stacked aromatic rings is considerably governed by the orbital interaction between the highest occupied molecular orbital of the indole ring and the lowest unoccupied one of the adeninium ring. The ring stacking observed in II was stabilized by the strong coupled dipole–dipole interaction. Absorption, fluorescence, and proton nuclear magnetic resonance spectra indicated the existence of a stacking interaction in the aqueous solutions of I and II, as well as in their crystalline states. The biological implication for the observed stacking interactions has been discussed.

The mutual recognition between protein and nucleic acid is specific and fundamental steps in the expression of cellular genome. This recognition is significantly guaranteed by the specific interaction between their constituent chemical groups [for a review, see Helene & Lancelot (1982)], as well as by the complementary spatial structure between these macromolecules (Carter & Kraut, 1974; Church et al., 1977; Warrant & Kim, 1978; Steitz et al., 1982; Gabbay et al., 1976).

The interaction mode of the indole ring with nucleic bases is important in understanding the role of the tryptophanyl residue in the protein associated with the nucleic acid. The indole ring of the best π-electron-donating group among the amino acids (Pullman & Pullman, 1958) is preferentially associated with the nucleic bases by π–π stacking interaction [for example, see Helene & Lancelot (1982) and Helene & Maurizot (1981)]. In some proteins, indeed, the stacking interaction of the tryptophanyl residue is essential for the binding with nucleic acids or nucleotides: gene 32 protein–poly(1-N^6-ethenoadenylic acid) (Toulme & Helene, 1980) or –DNA (Helene et al., 1976), creatine kinase–adenosine 5′-diphosphate (ADP)[1] or –adenosine 5′-triphosphate (ATP) (Vasak et al., 1979), phenylalanyl-tRNA synthetase–transfer RNA (Lefevre et al., 1980), glutamate dehydrogenase–ADP (Jallon et al., 1973), and meromycin–ATP, –guanosine 5′-triphosphate, or –uridine 5′-triphosphate (Yoshino et al., 1972). Since adenine base is a constituent of biologically important coenzymes such as flavin adenine dinucleotide and nicotinamide adenine dinucleotide, the detailed study on the stacking mode with the indole ring would also provide useful information on the binding mode of these coenzymes to apoenzymes. The indole ring is known to stack preferentially with adenine rather than pyrimidine bases in solution (Wagner & Lawaczeck, 1972; Mutai et al., 1975), but no such interaction has yet been detected in crystals. As far as we know, four kinds of crystal structures have been reported as models for adenine–indole interaction: 3-(3-adenin-9-ylpropyl)tryptamine (Ohki et al., 1977a,b), 9-(3-indol-3-ylpropyl)adenine (IC3A) (Bunick & Voet, 1982), 9-ethyladenine–indole (1:1) complex (Kaneda & Tanaka, 1976), and adenine-9-acetic acid–tryptamine (1:1) complex (Ishida et al., 1979). In these crystals, a hydrogen bond was formed between the indole NH group and the adenine moiety. However, no stacking interaction was observed between the indole and adenine rings. In general, the stacking interaction arises from the interaction between the π-orbitals of two aromatic rings, and particularly, the interaction between the highest occupied molecular orbital (HOMO) of the donor ring and the lowest unoccupied molecular orbital (LUMO) of the acceptor ring is important.

When adenine base takes the adeninium form by protonation in acidic conditions (pK_a = 4.1) or by methylation with methyltransferases or alkylating agents, the prominent stacking with the indole ring is expected. In this case, the LUMO energy of adenine [0.1367 atomic unit (au)] is significantly lowered by the quarternization of the base nitrogen atom, e.g., –0.1182 au for N(1)-protonated adenine. The N(1)-protonation of adenine base saves energy of 0.2549 au (ca. 159.95 kcal/mol) in the interaction with the HOMO of the indole ring (its energy is value –0.3996 au). Despite the extensive electrostatic repulsion, the stacking interaction between indole and adenine rings has been observed in acidic solution of the dinucleoside monophosphate containing adenine base–L-tryptophan (Kolodny et al., 1977) or –tryptamine (Kolodny & Neville, 1980) and adenosine–tryptophan (Dimicoli & Helene, 1973) systems.

On the basis of these factors, we surveyed model systems suitable for X-ray crystallographic and spectroscopic studies and then selected 1,9-dimethyladeninium $(DMA)^+$–indole-3-acetate (IAA^-) complex (model I) and 9-(3-indol-3-ylpropyl)-1-methyladeninium ($IC3MA^+$) iodide (model II) as an inter- or intramolecular stacking model for adeninium–indole interaction. Figure 1 shows the chemical formulas of

† From the Department of Physical Chemistry, Osaka College of Pharmacy, 2-10-65 Kawai, Matsubara-City, Osaka 580, Japan. *Received February 11, 1983.* This work is part 10 of the series "Structural Studies of the Interaction between Indole Derivatives and Biologically Important Aromatic Compounds".

[1] Abbreviations: ADP, adenosine 5′-diphosphate; ATP, adenosine 5′-triphosphate; IC3A, 9-(3-indol-3-ylpropyl)adenine; HOMO, highest occupied molecular orbital; LUMO, lowest unoccupied molecular orbital; DMA^+, 1,9-dimethyladeninium; IAA, indole-3-acetic acid; $IC3MA^+$, 9-(3-indol-3-ylpropyl)-1-methyladeninium; CNDO/2, complete neglect of differential overlap; ^1H NMR, proton nuclear magnetic resonance; DSS, 4,4-dimethyl-4-silapentane-1-sulfonate.

0006-2960/83/0422-3571$01.50/0

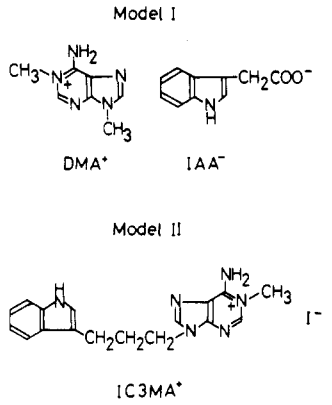

FIGURE 1: Model compounds used for studies on adeninium–indole interaction.

both the models. Model I would give the information about the strength of the stacking interaction, whereas model II provides the knowledge of the geometrical requirement of the interaction. The preliminary X-ray result was already reported (Ishida & Inoue, 1981a; Ishida et al., 1982). Herein, we describe the details of the crystallographic and spectroscopic studies, which would provide valuable information for the interaction between the tryptophanyl residue of protein and the N(1)-methylated or -protonated adenine base of nucleic acid.

Experimental Procedures

Synthesis and Crystallization. 9-Methyladenine was synthesized from adenine and trimethyl phosphate (Yamauchi et al., 1976) and recrystallized from ethanol–water (1:4) (mp 280–281 °C). DMA^+I^- was synthesized by the reaction of methyl iodide and 9-methyladenine by reference to the methylation of adenosine (Jones & Robins, 1963) and recrystallized from ethanol–water (1:1) (mp >310 °C). DMA^+I^- dissolved in water (ca. 1% solution) was converted to the OH^- form by using a column of Amberlite IRA-401 anion-exchange resin. Equimolar quantities of IAA dissolved in ethanol were added to the solution. The mixed solution was evaporated to dryness under vacuum, and then, the residue was dissolved in a water–dioxane (1:1) mixture. Transparent, brownish platelet crystals were obtained from the solution (2×10^{-4} M) by slow evaporation at room temperature. The absorption spectrum of the crystals dissolved in water indicated that they are constituted of an equimolar ratio of the component DMA^+ and IAA^- molecules, and the thermal analysis of the crystals showed the existence of three crystalline waters per one complex pair.

On the other hand, IC3A was prepared from indole-3-propionic acid and adenine according to the published method (Mutai et al., 1975). After the solution of 0.1 g of IC3A, 0.1 mL of methyl iodide, and 0.3 mL of *N,N'*-dimethylacetamide was stirred for 24 h at room temperature, 1.5 mL of acetone was added to the solution, yielding the light brownish precipitates of $IC3MA^+I^-$ (mp 269–270 °C). The pale brownish platelet crystals were obtained from the aqueous solution by slow evaporation at room temperature. Thermal analysis indicated that the crystals contain two waters per one molecule.

X-ray Data Collection. A single crystal with dimensions of ca. 0.4 × 0.2 × 0.3 mm (model I) or 0.3 × 0.1 × 0.5 mm (model II), sealed in a glass capillary tube under the presence of some mother liquids, was used for X-ray studies. Preliminary oscillation and Weissenberg photographs showed that model I is monoclinic and in space group $P2_1/c$ from its systematic absences and that model II is triclinic and in space group $P1$ or $P\bar{1}$. The space group of model II was finally determined to be centrosymmetric $P\bar{1}$ from the statistical distribution of normalized structure factors (E) (Karle et al., 1965). The densities of both crystals were measured by the flotation method in a mixture of benzene and carbon tetrachloride. The cell constants were determined on a four-circle diffractometer (Rigaku Denki Co., Japan) by using the 25 reflections with 2θ values ranging from 50 to 60° and refined by the least-squares method. Table I summarizes the crystallographic data.

Table I: Crystal Data for Models I and II

	model I	model II
chemical formula	$C_7H_{10}N_5^-\cdot C_{10}H_8NO_2^+\cdot 3H_2O$	$C_{17}H_{19}N_6I\cdot 2H_2O$
mol wt	392.41	470.31
crystal system	monoclinic	triclinic
space group	$P2_1/c$	$P\bar{1}$
cell constants		
a (Å)	7.216 (2)	12.199 (5)
b (Å)	21.004 (9)	11.923 (6)
c (Å)	12.679 (5)	7.449 (3)
α (deg)		95.88 (5)
β (deg)	91.18 (2)	97.88 (5)
γ (deg)		67.31 (3)
vol (Å^3)	1921 (2)	988.7 (8)
Z	4	2
D_m (g·cm^{-3})	1.353 (1)	1.555 (2)
D_x (g·cm^{-3})	1.357	1.580
μ (Cu Kα)(cm^{-1})	8.14	130.49
F(000)	832	472

Three-dimensional intensity data were collected up to a 2θ limit of 130° by the same diffractometer by employing graphite-monochromated Cu Kα radiation with an $\omega - 2\theta$ (model I) or ω (model II) scan technique with a scan speed of 4° min^{-1} and a scan width of $1.0 + 0.15 \tan\theta$ (model I) or $1.4 + 0.15 \tan\theta$ (model II) in 2θ; the background was counted for 5 s at the both edges of each reflection. The intensities of four standard reflections, monitored at 50 reflection intervals, revealed no structural deterioration during the data collection. The measured 3288 (model I) or 3367 (model II) independent intensities were corrected by Lorentz and polarization factors.

Structure Solution and Refinements. The structure of model I was solved by the direct method with the program MULTAN 78 (Main et al., 1978): a correct phase set of 212 $|E|$'s (>1.86) gave an E map in which all non-hydrogen atoms could be positioned in reasonable chemical sense. On the other hand, the crystal structure of model II was solved by Patterson–Fourier methods: the position of the iodide ion was indicated on a three-dimensional Patterson function, and the positions of remaining non-hydrogen atoms were found by successive Fourier syntheses.

The positional parameters were refined by the full-matrix least-squares method with isotropic thermal parameters and then by the block-diagonal least-squares method with anisotropic temperature factors. A difference Fourier map was then computed, and the geometrically reasonable hydrogen atoms were found, except for those of waters in model I. They were included in all subsequent refinements with isotropic temperature factors. The function minimized was $\sum w(|F_o| - |F_c|)^2$. The final least-squares refinement was computed with a weighting scheme as follows: (model I) $w = 0.22724$ for $F_o = 0.0$, $w = 1.0/[\sigma F_o^2 - 0.30720|F_o| + 0.01031|F_o|^2]$ for $F_o > 0.0$; (model II) $w = 0.60986$ for $F_o = 0.0$, $w = 1.0/[\sigma F_o^2 -$

[2] UV absorption and fluorescence spectra for the IC3A molecule were measured by Mutai et al. (1975), and the prominent stacking interaction was reported to exist in a dilute solution.

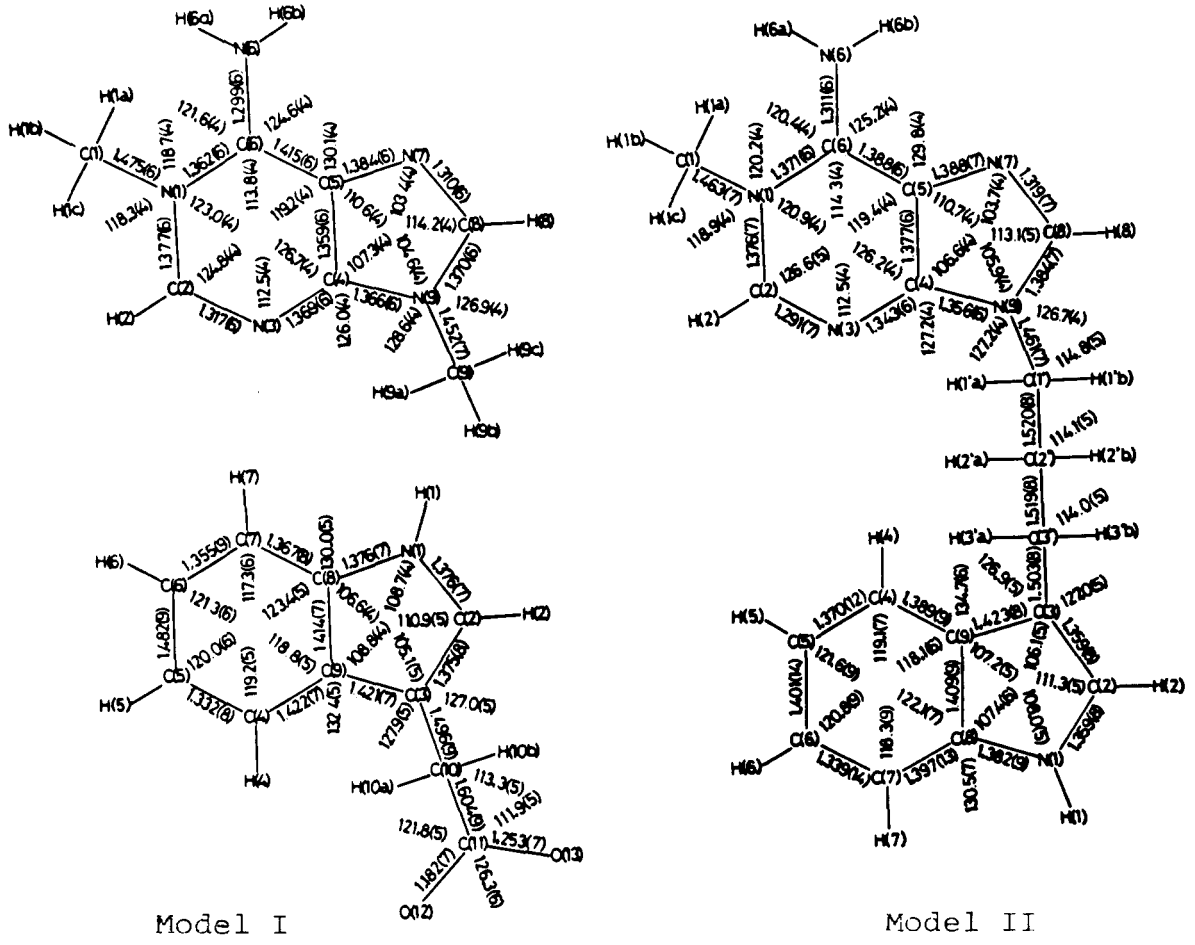

FIGURE 2: Bond lengths (Å) and angles (deg) between non-hydrogen atoms with their standard deviations in parentheses. The figure also shows the atomic numbering used in this work.

$0.00863|F_0| + 0.00625|F_0|^2]$; σF_0 is the standard deviation based on counting statistics. In the final refinement, none of the positional parameters shifted more than one-third of their standard deviations. The final R (R_w) value was 0.103 (0.122) or 0.062 (0.110) for model I or II, respectively. The atomic parameters with the estimated standard deviations are given in Table II (see paragraph at end of paper regarding supplementary material). For all crystallographic computations, the UNICS (1979) programs were used; the atomic scattering factors used were those published by Cromer & Waber (1974).

Molecular Orbital Calculations. The molecular orbital calculations of DMA^+ and 3-methylindole were carried out by using their standard coordinates (Taylor & Kennard, 1982a; Ishida, 1979) and the molecular orbital CNDO/2 (complete neglect of differential overlap) method (Pople & Segal, 1966). The electronic energy was converged by the iterative SCF (self-consistent field) method.

UV Absorption and Fluorescence Emission Spectra. UV absorption spectra in the range 220–340 nm were measured at 25 °C on a Hitachi 624 spectrometer in 10-mm cells. The relative quantum efficiency of fluorescence was determined on a Hitachi-650-40 spectrofluorometer with a xenon lamp. The emission spectra were measured at 25 °C with 295-nm excitation and, then, were not corrected for monochromater efficiency and photomultiplier response. The absorption and fluorescence spectra were measured 3 times by using 6.0×10^{-5} M sample solution in 0.025 M phosphate buffer containing 10% ethanol (pH 7.1).

^1H NMR Spectra. The 90-MHz ^1H NMR spectra were recorded at 0.2 M sample concentration in 50% $C^2H_3O^2H$–^2H_2O solution on a Hitachi Perkin-Elmer spectrometer. The chemical shifts were determined from internal 4,4-dimethyl-4-silapentane-1-sulfonate (DSS). All numerical calculations were carried out on an ACOS-900 computer at the Computation Center of Osaka University.

Results and Discussion

Descriptions of Molecular Structures. Figure 2 shows the bond lengths and angles for non-hydrogen atoms. The averaged standard deviations for lengths and angles are 0.006 Å and 0.3° for model I and 0.007 Å and 0.5° for model II, respectively. Although some values are different between both models, these values are normal as judged by the values of adeninium (Taylor & Kennard, 1982b) and indole (Ishida, 1979) compounds. As pointed out by Taylor & Kennard (1982b), the quaternization at the N(1) atom caused the elongation of the N(1)–C(2) bond length and the expansion of the C(6)–N(1)–C(2) angle in comparison with the corresponding values of neutral adenine [=1.338 (3) Å and 118.8 (2)°, respectively]. Reversely, the contractions of the C(2)–N(3) length and the N(1)–C(2)–N(3) and N(1)–C(6)–C(5) angles were induced by the quaternization [these averaged values in neutral adenine are 1.332 (2) Å and 129.0 (1) and 117.6 (1)°, respectively].

Table III lists the least-squares planes for the adeninium, indole, and carboxyl (of model I) moieties and the displacements of individual atoms from these planes. Both adeninium rings are almost planar with a maximum shift of −0.026 (5) (model I) or 0.023 (5) Å (model II) at the C(5) atom: the root mean square deviations (rmsd's) of respective nine non-hydrogen atoms from their best fit planes are both 0.008 Å. On the other hand, the indole ring in model II has the relatively

Table II: Positional ($\times 10^4$) and Isotropic Thermal Parameters of Non-Hydrogen Atoms with Their Estimated Standard Deviations of Models I and II

atom	x	y	z	B^a
		Model I		
DMA^+				
N(1)	9519 (5)	3082 (2)	4593 (3)	4.3 (2)
C(1)	10067 (7)	2656 (2)	5467 (3)	4.8 (3)
C(2)	8959 (7)	2812 (2)	3651 (3)	4.6 (3)
N(3)	8400 (5)	3134 (2)	2813 (3)	4.5 (2)
C(4)	8455 (6)	3778 (2)	2970 (3)	4.4 (3)
C(5)	8990 (6)	4084 (2)	3868 (3)	3.9 (3)
C(6)	9595 (6)	3723 (2)	4750 (3)	4.0 (3)
N(6)	10133 (6)	3964 (2)	5647 (3)	4.3 (2)
N(7)	8919 (5)	4737 (2)	3727 (3)	4.8 (3)
C(8)	8331 (6)	4799 (2)	2751 (4)	4.7 (3)
N(9)	8020 (5)	4234 (2)	2239 (3)	4.5 (3)
C(9)	7353 (8)	4150 (3)	1162 (4)	6.2 (4)
IAA^-				
N(1)	4609 (6)	2603 (2)	9638 (3)	6.3 (3)
C(2)	5219 (7)	2474 (3)	10648 (4)	5.6 (4)
C(3)	5197 (7)	1830 (3)	10842 (4)	5.8 (4)
C(4)	4252 (7)	905 (3)	9579 (4)	6.6 (4)
C(5)	3633 (8)	780 (3)	8607 (5)	7.3 (5)
C(6)	3260 (8)	1309 (3)	7859 (4)	7.1 (5)
C(7)	3531 (8)	1924 (3)	8144 (4)	6.1 (4)
C(8)	4173 (7)	2037 (3)	9146 (4)	5.1 (3)
C(9)	4550 (6)	1549 (2)	9886 (3)	4.4 (3)
C(10)	5764 (7)	1502 (3)	11843 (4)	6.1 (4)
C(11)	4047 (7)	1323 (3)	12569 (4)	5.2 (3)
O(12)	2503 (4)	1440 (2)	12310 (2)	5.6 (2)
O(13)	4569 (5)	1082 (2)	13428 (3)	8.9 (4)
waters of crystn				
O(1)W[b]	9882 (5)	3700 (2)	8831 (3)	6.3 (3)
O(2)W	2637 (6)	4231 (2)	10127 (3)	8.5 (4)
O(3)W	7587 (6)	4716 (2)	8524 (3)	8.4 (4)
		Model II		
I	6506 (4)	3318 (3)	2754 (6)	5.4 (0)
N(1)A[b]	8418 (4)	7593 (4)	8195 (6)	3.3 (2)
C(1)A	9087 (5)	6305 (5)	8523 (8)	4.2 (3)
C(2)A	7281 (4)	7940 (5)	7305 (7)	3.6 (3)
N(3)A	6573 (4)	9033 (4)	6920 (6)	3.5 (2)
C(4)A	7070 (4)	9856 (4)	7464 (6)	3.0 (2)
C(5)A	8191 (4)	9621 (4)	8373 (6)	3.1 (2)
C(6)A	8922 (4)	8433 (4)	8765 (6)	3.0 (2)
N(6)A	10014 (4)	8089 (4)	9581 (7)	3.8 (2)
N(7)A	8424 (4)	10680 (4)	8684 (7)	4.0 (2)
C(8)A	7432 (5)	11526 (5)	7996 (9)	4.5 (3)
N(9)A	6579 (3)	11070 (4)	7223 (6)	3.5 (2)
C(1′)	5428 (4)	11746 (5)	6229 (8)	4.0 (3)
C(2′)	4582 (5)	12786 (5)	7327 (9)	4.6 (3)
C(3′)	4095 (5)	12378 (5)	8803 (8)	4.3 (3)
N(1)I[b]	2820 (5)	10031 (5)	7361 (8)	5.2 (3)
C(2)I	3705 (5)	10405 (6)	8137 (8)	4.6 (3)
C(3)I	3361 (4)	11631 (5)	8101 (7)	3.9 (3)
C(4)I	1330 (5)	13204 (7)	6786 (9)	5.5 (4)
C(5)I	235 (6)	13292 (9)	5929 (10)	6.9 (5)
C(6)I	−74 (6)	12269 (10)	5555 (11)	7.4 (5)
C(7)I	713 (7)	11158 (9)	5971 (11)	7.1 (5)
C(8)I	1842 (6)	11049 (6)	6817 (8)	4.9 (4)
C(9)I	2173 (5)	12064 (5)	7224 (7)	3.8 (3)
waters of crystn				
O(1)W	8075 (4)	4236 (5)	−43 (8)	6.0 (3)
O(2)W	3371 (5)	4721 (6)	3205 (8)	7.0 (4)

[a] The equivalent isotropic temperature factors for non-hydrogen atoms have been calculated by $B_{eq} = {}^4/_3(a^2B_{11} + b^2B_{22} + c^2B_{33} + 2abB_{12}\cos\gamma + 2acB_{13}\cos\beta + 2bcB_{23}\cos\alpha)$. [b] The suffixes W, A, and I in the atom designations refer to water molecules and adeninium and indole rings, respectively.

large fluctuation from its plane (rmsd = 0.013 Å), compared with that in model I (rmsd = 0.008 Å). This may be due to the high thermal parameters of the former indole ring. The carboxyl group in model I is almost planar and exists in an anionic form in which the electronegative charge predominantly localizes on the O(12) atom. This group is approximately at right angles to the indole ring and has a dihedral angle of 82.2 (3)°.

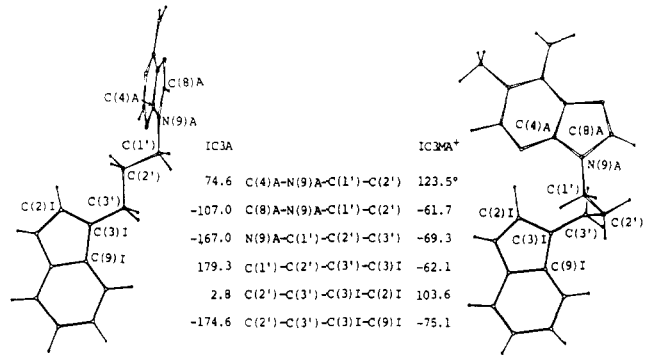

FIGURE 3: Conformational comparison between IC3A (left part) and $IC3MA^+$ (right part) molecules. Both molecular structures are projected on their indole rings, respectively.

The torsion angles χ [C(2)–C(3)–C(10)–C(11)] and ϕ [C(3)–C(10)–C(11)–O(12)] of the present IAA conformation are 98.4 (4)° and 0.7 (4)°, respectively. These values are in the range of (+) anti-clinal for χ and syn-periplanar for ϕ and are close to those of IAA alone [χ = 113.4°, ϕ = −11.7° (Karle et al., 1964)] and the complexed IAA with 5-methoxytryptamine [χ = 113.4, ϕ = −29.4° (Sakaki et al., 1976)], nicotinamide [χ = 80.4°, ϕ = −6.4° (Inoue et al., 1978)], and tyramine [χ = 113.3°, ϕ = −17.1° (Ishida & Inoue, 1981b)], suggesting the most energetically stable conformation for the IAA molecule.

The conformational comparison between $IC3MA^+$ and IC3A (Bunick & Voet, 1982) molecules is of interest in connection with the influence of N(1)-methylation on the molecular conformation (see Figure 3). The large difference is seen in the torsion angles of the propylene group connecting both aromatic rings; both the torsion angles N(9)A–C(1′)–C(2′)–C(3′) and C(1′)–C(2′)–C(3′)–C(3)I of the $IC3MA^+$ molecule lie in a gauche$^-$ region, while those of IC3A molecule are in a trans one. Consequently, $IC3MA^+$ and IC3A molecules take a folded and a fully extended conformation, respectively. We also note that the adenine ring of IC3A molecule takes almost right angles to the indole ring (dihedral angle = 83.5°) and that of the $IC3MA^+$ molecule is almost parallel to the indole ring [dihedral angle = 2.1 (1)°]. The IC3A molecule is stabilized by the hydrogen-bond formation between the neighboring polar atoms. In contrast, the prominent stacking interaction between the indole and adeninium rings stabilizes the crystal structure of the $IC3MA^+$ molecule (discussed later). Therefore, the different interaction mode of the aromatic rings probably contributes to the conformational difference between IC3A and $IC3MA^+$ molecules.

Descriptions of Crystal Structures. Figure 4 shows the stereoscopic views of the crystal packings in models I and II, viewed along the *b* axis. The filled and open circles represent the iodide ions and the oxygen atoms of waters, respectively. The layers consisting of the alternative stacking of adeninium and indole rings are piled up to the *a* (model I) or *c* axis (model II). These layers are stabilized by many hydrogen bonds or short contact formations between the polar atoms of neighboring molecules and via waters of crystallization or iodide existing among these layers. The networks of hydrogen bonds for both models are shown in Figure 5. Table IV summarizes the hydrogen-bonding parameters and short contacts. All hydrogen bonds fall within the ranges observed for such interactions (Ondik & Smith, 1968). The centrosymmetrically related adeninium rings in both models are linked to each other by two N(6)–H···N(7) hydrogen bonds. This hydrogen-

Table III: Least-Squares Planes and Deviations of Atoms (Å) from Planes

(A) Equations of Best Planes Expressed by $m_1X + m_2Y + m_3Z = d$ in Orthogonal Space

plane	m_1	m_2	m_3	d
model I				
adeninium ring	0.948 84	0.011 77	−0.315 54	4.639 52
indole ring	0.946 75	0.060 57	−0.316 21	1.474 65
carboxyl group	0.057 72	−0.905 17	0.421 11	−2.767 56
model II				
adeninium ring	−0.468 53	0.097 42	0.878 06	0.037 93
indole ring	−0.445 50	0.073 06	0.892 30	2.384 38

(B) Deviations from Best Planes[a]

model I			model II	
adeninium ring	indole ring	carboxyl group	adeninium ring	indole ring
N(1)* 0.004 (4)	N(1)* 0.006 (5)	C(10)* 0.007 (9)	N(1)* −0.010 (5)	N(1)* −0.013 (7)
C(2)* 0.014 (5)	C(2)* 0.009 (6)	C(11)* −0.019 (6)	C(2)* −0.013 (6)	C(2)* 0.003 (7)
N(3)* −0.005 (5)	C(3)* −0.007 (6)	O(12)* 0.003 (5)	N(3)* 0.007 (5)	C(3)* 0.011 (7)
C(4)* −0.018 (5)	C(4)* 0.003 (6)	O(13)* 0.005 (7)	C(4)* 0.010 (5)	C(4)* −0.001 (9)
C(5)* −0.026 (5)	C(5)* 0.010 (7)	C(3) 0.074 (11)	C(5)* 0.023 (5)	C(5)* −0.017 (11)
C(6)* 0.006 (5)	C(6)* 0.006 (8)	H(10a) 0.75 (5)	C(6)* 0.005 (5)	C(6)* 0.017 (12)
N(7)* 0.002 (5)	C(7)* −0.009 (7)	H(10b) −0.93 (5)	N(7)* −0.010 (6)	C(7)* 0.018 (12)
C(8)* 0.016 (5)	C(8)* −0.011 (6)		C(8)* −0.010 (7)	C(8)* 0.010 (8)
N(9)* 0.006 (5)	C(9)* −0.006 (5)		N(9)* −0.008 (5)	C(9)* −0.011 (6)
C(1) −0.003 (6)	C(10) −0.003 (9)		C(1) −0.026 (7)	C(3′) 0.011 (9)
N(6) −0.001 (6)	H(1) −0.13 (5)		N(6) −0.018 (6)	H(1) 0.15 (11)
C(9) 0.005 (7)	H(2) 0.17 (5)		C(1′) −0.110 (7)	H(2) 0.12 (7)
H(2) 0.09 (4)	H(4) −0.16 (5)		H(2) −0.08 (7)	H(4) −0.11 (7)
H(8) −0.05 (5)	H(5) −0.08 (6)		H(8) 0.18 (7)	H(5) −0.19 (9)
	H(6) −0.02 (5)			H(6) −0.20 (9)
	H(7) −0.12 (4)			H(7) 0.04 (13)

[a] Atoms with asterisks define the plane in each case.

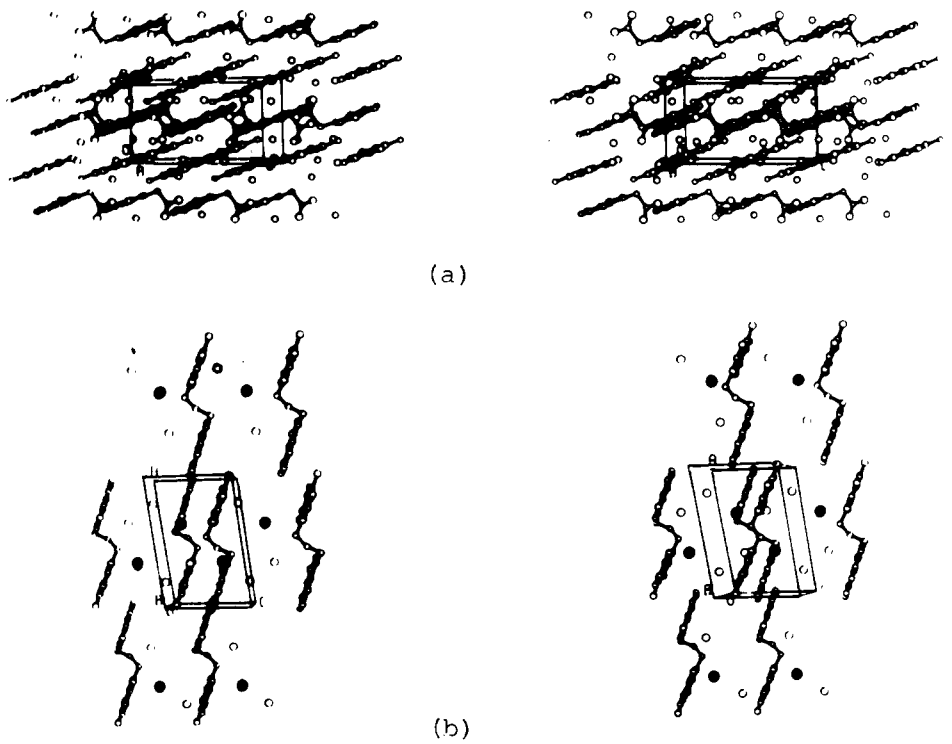

FIGURE 4: Stereoscopic packing diagrams of models I (a) and II (b) viewed down the *b* axis. The full and open circles represent iodide ions and waters of crystallization, respectively.

bonding mode has frequently been observed in N(1)-protonated or -methylated adeninium compounds such as adenine hydrochloride (Tavale et al., 1969) or DMA^+Cl^- (Chiang et al., 1979). The absence of an N(3) atom for hydrogen bonding may imply the poor proton-accepting ability of this atom in comparison with that of the N(7) atom. The N(6) atom is hydrogen bonded to the O(12) (model I) or O(1)W (model II) atom. The N(1) atom of IAA^- in model I is hydrogen bonded to the neighboring O(13) atom of the same molecule, and two oxygen atoms [O(12) and O(13)] of the carboxyl group are further linked to water molecules. On the other hand, the indole ring of model II does not participate in hydrogen-bond formation but in N–H···I^- short contact with relatively long distance. The water molecules were linked to the neighboring polar atoms by the hydrogen bonds or by O–H···I^- short contacts with reasonable distances.

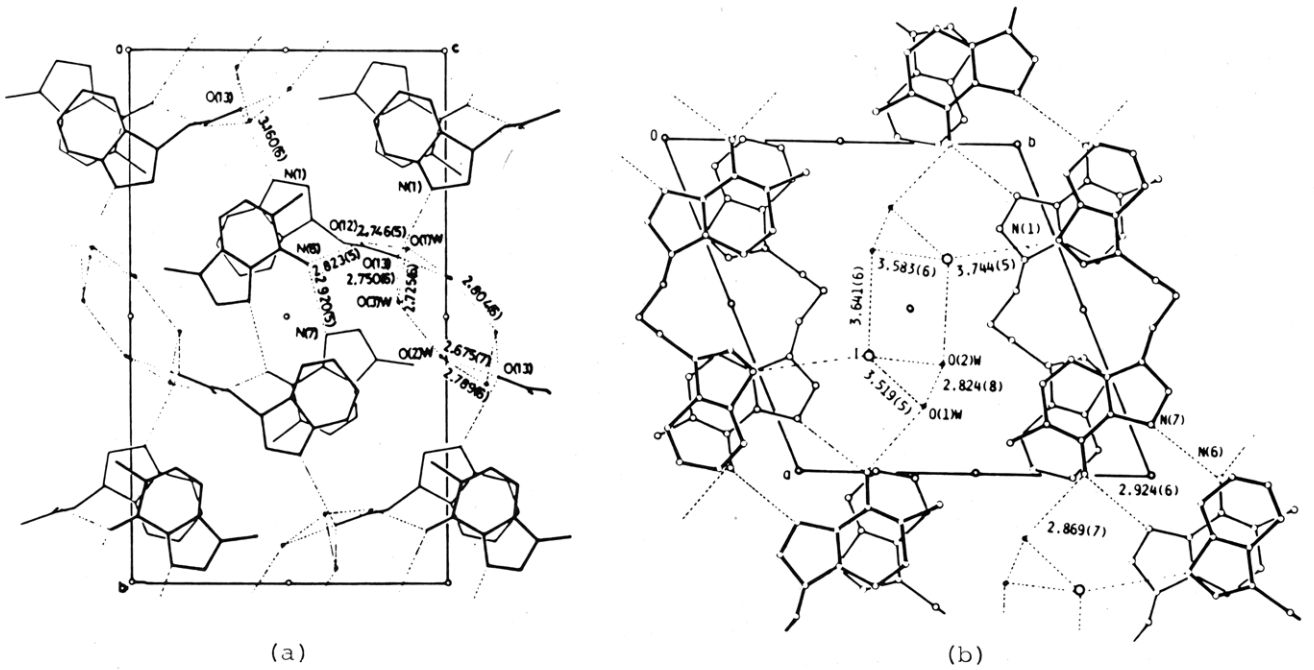

FIGURE 5: Crystal packing modes of models I (a) and II (b). Dotted lines represent possible hydrogen bonds for model I and hydrogen bonds and N–H···I or O–H···I short contacts for model II.

Stacking Interactions between Adeninium and Indole Rings. Figure 6 illustrates the stacking modes between the indole and adeninium rings in both models. The respective two stacked indole rings are related to each other by the *a* (model I) or *c*-axis (model II) translation operation. Both adeninium rings are almost parallel to the indole planes; their dihedral angles are 2.7 (2) and 2.1 (2)° for model I and II, respectively. The average interplanar spacing in the area of overlap are 3.497 and 3.351 Å for the upper and lower pairs (named stacks I and II) of model I and 3.431 and 3.476 Å for those (named stacks III and IV) of model II, respectively. Since the interplanar spacing of stacks I, III, and IV are all outside of the normal van der Waals separation distance (3.4 Å), these stacking interactions would be stabilized by the van der Waals contacts between the respective two aromatic rings. In stack II, however, such parallel stacking and short interplanar spacing (<3.4 Å) indicate that the two aromatic rings are partly associated by the π–π charge transfer from the occupied orbital of the indole ring to the unoccupied one of the adeninium ring.

It is a characteristic commonly found in these stacked pairs that the indole ring interacts with the pyrimidine portion of the adeninium ring more strongly than with the imidazole portion. Such an indole–pyrimidine stacking mode has been proposed for the serotonin–poly(adenylic acid) system, in which the ^{1}H NMR study by Helene et al. (1971) showed the upfield shift of adenine H(2) proton by virtue of indole–adenine ring current effect and the downfield shift of the H(8) proton by adenine–adenine destacking. As judged from the atomic charges calculated by the CNDO/2 method, the positive charge in the adeninium ring was not localized on the N(1) atom. Therefore, the preferential stacking interaction with the pyrimidine portion as shown in Figure 6 may be a characteristic feature in the adenine–indole system, as well as in the adeninium–indole one.

The crystal structures of the 9-ethyladenine–indole (1:1) complex (Kaneda & Tanaka, 1976) and IC3A (Bunick & Voet, 1982) have been reported as a simple model for the inter- and intramolecular interaction between adenine and indole rings, respectively. However, no apparent stacking interaction

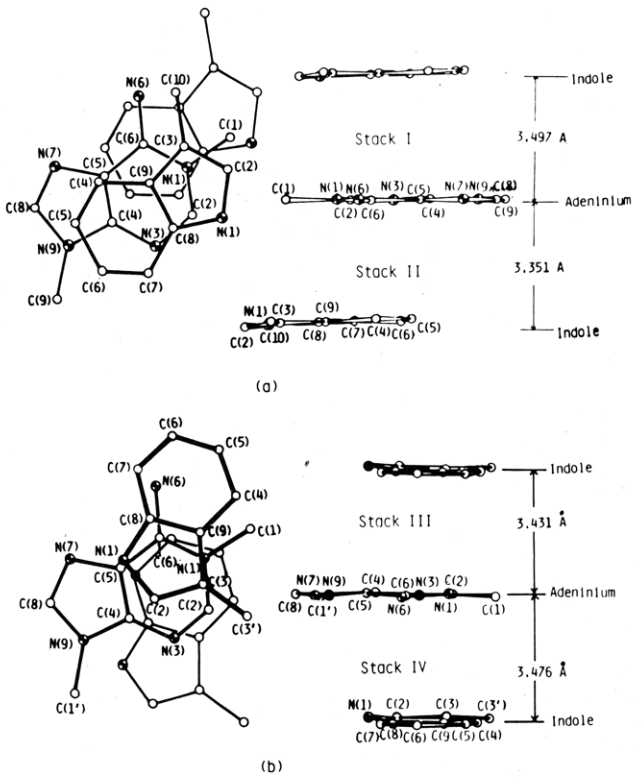

FIGURE 6: Stacking mode of nearest-neighboring indole–adeninium ring pairs, projected perpendicular (left part) or parallel (right part) to the central adeninium ring: (a) model I; (b) model II.

was observed in these cases. The N(1)-quaternization of the adenine ring appears to be indispensable for the prominent π–π stacking interaction with the indole ring. Probably, its stacking formation is largely due to the lowering of the LUMO energy of the adeninium ring.

Ring Orientation in Adeninium–Indole Stacking Interaction. It is well-known that the dipole (induced)–dipole (Lawaczeck & Wagner, 1974; Bugg et al., 1971) and electrostatic (Ash et al., 1977) interactions are largely responsible for specifying the mutual orientation of two associated molecules. Figure

Table IV: Hydrogen Bonds and Short Contacts with Their Standard Deviations

Hydrogen Bonds					
			distance (Å)		
donor	acceptor	symmetry code for acceptor	D-A	H-A	angle D-H···A (deg)
model I					
N(6)A	N(7)A	$2-x, 1-y, 1-z$	2.920 (5)	2.16 (5)	165 (5)
N(6)A	O(12)I	$1+x, y, z$	2.823 (5)	1.86 (4)	164 (4)
N(1)I	O(13)I	$x, {}^1/_2-y, -{}^1/_2+z$	3.160 (6)	2.25 (5)	160 (4)
O(1)W	O(12)I	$1+x, y, z$	2.746 (5)		
O(1)W	O(3)W	x, y, z	2.725 (6)		
O(2)W	O(13)I	x, y, z	2.675 (7)		
O(2)W	O(1)W	$1+x, y, z$	2.789 (6)		
O(3)W	O(13)I	x, y, z	2.750 (6)		
O(3)W	O(2)W	$1-x, 1-y, 2-z$	2.804 (6)		
model II					
N(6)A	N(7)A	$2-x, 2-y, 2-z$	2.924 (6)	1.88 (7)	159 (6)
N(6)A	O(1)W	$2-x, 1-y, 1-z$	2.869 (7)	2.05 (6)	141 (8)
O(1)W	O(2)W	$1-x, 1-y, -z$	2.824 (8)	1.80 (9)	179 (8)

N-H···I or O-H···I Short Contacts					
			distance (Å)		
donor	acceptor	symmetry code for acceptor	D-A	H-A	angle D-H···A (deg)
model II					
N(1)I	I	$1-x, 1-y, 1-z$	3.744 (5)	3.00 (9)	154 (8)
O(1)W	I	x, y, z	3.519 (5)	2.61 (8)	151 (8)
O(2)W	I	x, y, z	3.583 (6)	2.58 (8)	179 (9)
O(2)W	I	$1-x, 1-y, 1-z$	3.641 (6)	3.09 (8)	165 (9)

Short Contacts Less Than 3.5 Å			
atom at x, y, z	atom	symmetry code for atom	distance
model I			
N(1)A	C(7)I	$1-x, y, z$	3.462 (7)
N(1)A	C(8)I	$1+x, y, z$	3.427 (6)
C(1)A	C(8)I	$1+x, y, z$	3.495 (7)
C(1)A	O(12)I	$1+x, y, z$	3.467 (6)
C(2)A	C(7)I	$1+x, y, z$	3.419 (8)
C(4)A	C(6)I	$1+x, y, z$	3.479 (8)
C(5)A	C(5)I	$1+x, y, z$	3.386 (7)
C(5)A	C(6)I	$1+x, y, z$	3.461 (8)
C(6)A	C(4)I	$1+x, y, z$	3.461 (7)
C(6)A	C(5)I	$1+x, y, z$	3.444 (7)
N(6)A	C(4)I	$1+x, y, z$	3.303 (7)
O(1)W	C(11)I	$1+x, y, z$	3.435 (7)
O(1)W	O(13)I	$1+x, y, z$	3.462 (6)
C(2)A	O(1)W	$x, {}^1/_2-y, -{}^1/_2+z$	3.253 (6)
N(1)I	C(11)I	$x, {}^1/_2-y, -{}^1/_2+z$	3.482 (7)
N(6)A	C(8)A	$2-x, 1-y, 1-z$	3.470 (6)
C(8)A	O(12)I	$1-x, 1-y, 1-z$	3.499 (6)
model II			
C(1)A	O(1)W	$2-x, 1-y, 1-z$	3.322 (8)
C(1)A	O(1)W	$x, y, 1+z$	3.464 (8)
N(3)A	C(1′)	$1-x, 2-y, 1-z$	3.472 (7)
C(5)A	N(1)I	$1-x, 2-y, 2-z$	3.493 (7)
C(6)A	C(8)I	$1-x, 2-y, 2-z$	3.473 (9)
N(6)A	C(7)I	$1-x, 2-y, 2-z$	3.486 (11)

7 and Table V summarize some parameters concerning the stacking orientations observed in both models. The vectors for the calculated permanent dipole moments of DMA^+ (A) and 3-methylindole (I) in their ground states are indicated by arrows above the respective structures (see Figure 7). The strong coupling of their permanent dipole moments shows that dipole–dipole interaction contributes to specifying the mutual orientation between the adeninium and indole rings in stacks III and IV. Such dipole–dipole coupling has also been observed in 1-(2-indol-3-ylethyl)-3-carbamoylpyridinium chloride (Herriott et al., 1974), an intramolecular stacking model for indole–pyridine coenzyme interaction. On the contrary, this interaction force is not strong in stacks I and II. The directions of their aromatic dipole moments are almost at right angles to each other, indicating the absence of dipole–dipole interaction. On the other hand, the electrostatic interaction does not appreciably operate in their ring orientations, and the electrostatic repulsions rather act on the short contact pairs as shown in Table V. The total electronic energies for the respective stacked pairs have positive values, because of the positive charge of the adeninium ring. However, stack III (its energy is 14.63 kcal/mol) is lower than the others, indicating an electrostatically favorable form of stack III.

The stabilization energies by stacking interactions are in the range from −38.7 to −41.3 kcal/mol, and these negative values imply that the stacking forces (van der Waals, charge transfer, and so on) overcome the effect of electrostatic repulsions. Since the stacking interaction is significantly dependent upon the π–π orbital interaction, it is important to investigate the orbital relationship between the HOMO of the indole ring and the LUMO of the adeninium ring. The results calculated by the CNDO/2 method are also given in Table V. In model I, stack II (Figure 7b) would be first formed by the orbital interactions between the HOMO (indole) and the LUMO

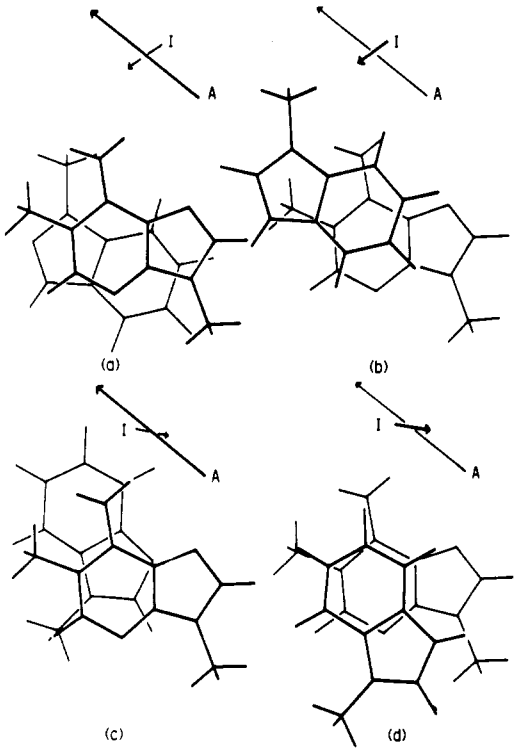

FIGURE 7: Stacking mode of indole–adeninium rings, viewed perpendicular to the adeninium plane. The vectors of permanent dipole moments [their values are 8.54 D for 1,9-dimethyladeninium cation (A) and 1.94 D for 3-methylindole (I), respectively] are represented by arrows above the respective figures. The letters in parentheses, a–d, correspond to the interaction modes listed in Table V.

(adeninium), because many short contact pairs in this stack have the same signs in their atomic coefficients. This indicates the possibility of interactions between their atomic orbitals. Several short contact pairs exhibiting orbital uncouplings are presumably attributable to the planarities of both aromatic rings. On the other hand, the atomic orbital interactions are observed in stack I (Figure 7a) of model I: the atomic coefficients between the HOMO of the indole ring and the LUMO of the adeninium ring of stack II also have the same signs in many short contact pairs. These results imply that stack I would be secondarily formed after the formation of stack II in the crystal packing of model I. Similarly, this relationship is applied to the ring stackings in model II. Six out of eight short contact pairs less than 3.6 Å in stack III (Figure 7c) have the same signs in their atomic coefficients, and further, the respective atoms in the short contact pairs of stack IV are interactable between the HOMO of the indole ring and the LUMO of the adeninium ring of stack III. The results reflect that stack III is primarily formed, and then, the formation of stack IV is accompanied in the crystal packing of model II. Therefore, the ring orientation in model II is also determined by the HOMO–LUMO interaction between their aromatic rings, besides the dipole–dipole one. It is worthwhile to note that while the rotation of the indole ring in stack III or IV by 180° about its dipole axis also satisfies the condition of dipole–dipole interaction, the HOMO–LUMO interaction does not permit this ambiguousness.

Ring Interaction of Models I and II in Solution. In order to investigate the stacking interaction of models I and II in solution, we measured UV absorption and fluorescence emission spectra for model II along with those of IC3A and their component molecules, i.e., 3-methylindole, DMA^+I^-, and 9-methyladenine. For model I together with those of DMA^+I^- and IAA, fluorescence emission and ^1H NMR spectra were

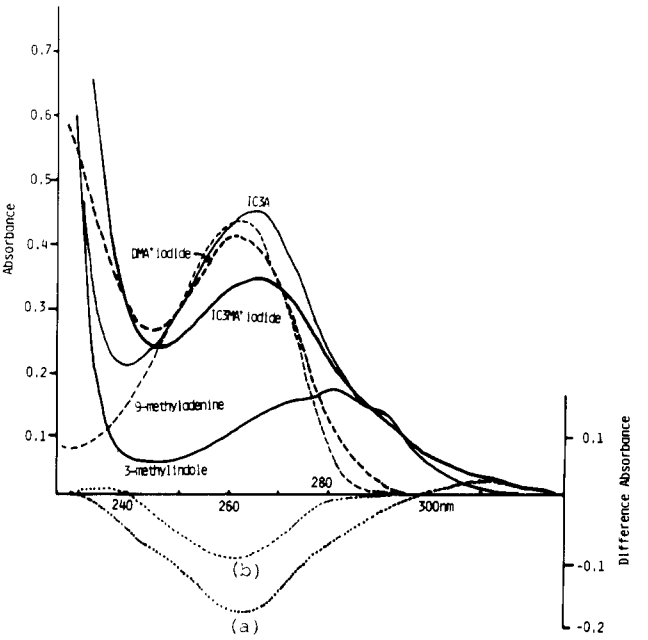

FIGURE 8: UV absorption spectra of $IC3MA^+I^-$, IC3A, DMA^+I^-, 9-methyladenine, and 3-methylindole and the difference spectra of $IC3MA^+I^-$ against DMA^+I^- plus 3-methylindole (a) and IC3A against 9-methyladenine plus 3-methylindole (b).

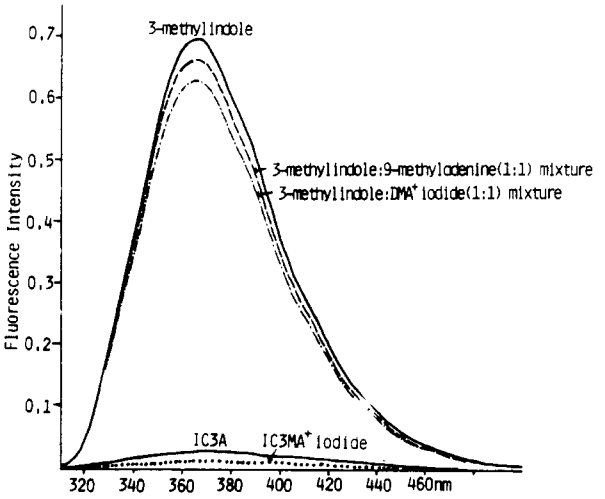

FIGURE 9: Fluorescence emission spectra of $IC3MA^+I^-$, IC3A, and 3-methylindole alone and coexisting with equimolar amounts of DMA^+I^- or 9-methyladenine: excitation 295 nm, wavelength scale 310–520 nm.

measured. Figure 8 shows the difference spectra of $IC3MA^+I^-$ and IC3A molecules against their component molecules. The negative band at 230–298 nm (model I) or 240–290 nm (IC3A) is caused by the hypochromic effects, indicating the intra- and/or intermolecular interaction between the indole and adeninium or adenine rings in the dilute solutions.[2] The larger hypochromic effect of $IC3MA^+$ than of IC3A suggests the existence of the stronger stacking interaction for the former molecule and the importance of the N(1)-quaternization of the adenine ring. Furthermore, the positive broad band at λ_{max} = 313 nm observed only in the former molecule could be assigned to be the charge-transfer band from the indole ring to the adeninium ring (Slifkin, 1971).

Figure 9 shows the fluorescence emission spectra (excited at 295 nm) of model II. By a comparison of the fluorescence intensity of 3-methylindole at 370 nm, the fluorescence emissions of $IC3MA^+I^-$, IC3A, and 3-methylindole coexisting with DMA^+I^- or 9-methyladenine were quenched by ca. 99.8,

Table V: Some Parameters for Adeninium–Indole Stacking Interactions

name	interaction mode	interplanar spacing (Å)	dihedral angle (deg)	electrostatic energy (kcal/mol)[a]	stabilization energy (kcal/mol)[b]
Stacking Parameters for Stacked Aromatic Rings					
stack I	Figure 7a	3.497	2.8 (2)	18.809	−38.716
stack II	Figure 7b	3.351	2.8 (2)	17.814	−41.289
stack III	Figure 7c	3.431	2.1 (2)	14.627	−39.218
stack IV	Figure 7d	3.476	2.1 (2)	18.695	−39.218

Stacking Parameters for Short-Contact Atomic Pairs Less Than 3.6 Å

name	atom: adeninium	atom: indole	distance (Å)	atomic charges: adeninium	atomic charges: indole	electrostatic interaction[c]	atomic coefficients[d]: LUMO (adeninium)	atomic coefficients[d]: HOMO (indole)	orbital coupling[e]
stack I	N(1)	C(2)	3.600 (6)	−0.063	0.047	+	−0.4020	−0.4163	+
	N(1)	C(3)	3.533 (6)	−0.063	−0.028	−	−0.4020	−0.4870	+
	C(1)	C(2)	3.522 (7)	0.063	0.047	−	−0.0399	−0.4163	+
	C(2)	N(1)	3.513 (6)	0.226	−0.126	+	0.2998	0.4201	+
	C(2)	C(8)	3.537 (7)	0.226	0.096	−	0.2998	0.1753	+
	N(3)	C(7)	3.550 (7)	−0.165	−0.041	−	0.0796	−0.2933	−
	N(3)	C(8)	3.536 (6)	−0.165	0.096	+	0.0796	0.1753	+
	C(5)	C(4)	3.554 (7)	−0.039	0.008	+	−0.0877	0.3402	−
stack II	N(1)	C(7)	3.462 (7)	−0.063	−0.041	−	−0.4022	0.2933	−
	N(1)	C(8)	3.427 (6)	−0.063	0.096	+	−0.4022	−0.1753	+
	C(1)	N(1)	3.506 (7)	0.063	−0.126	+	−0.0389	−0.4201	+
	C(1)	C(8)	3.495 (7)	0.063	0.096	−	−0.0389	−0.1753	+
	C(2)	C(7)	3.419 (8)	0.226	−0.041	+	0.3004	0.2933	+
	C(4)	C(6)	3.479 (8)	0.217	0.014	−	−0.4844	0.3012	−
	C(5)	C(5)	3.386 (7)	−0.039	−0.012	−	−0.0847	−0.1078	+
	C(5)	C(6)	3.461 (8)	−0.039	0.014	+	−0.0847	0.3012	−
	C(6)	C(4)	3.461 (7)	0.318	0.008	−	−0.5709	−0.3402	+
	C(6)	C(5)	3.444 (7)	0.318	−0.012	+	−0.5709	−0.1078	+
	N(6)	C(4)	3.303 (7)	−0.213	0.008	+	−0.2700	−0.3402	+
	N(6)	C(9)	3.518 (6)	−0.213	−0.013	−	−0.2700	−0.0908	+
	N(7)	C(5)	3.578 (7)	−0.164	−0.012	−	−0.1821	−0.1078	+
stack III	N(1)	C(3)	3.570 (7)	−0.063	−0.028	−	0.4022	−0.4870	−
	N(1)	C(9)	3.534 (7)	−0.063	−0.013	−	0.4022	0.0908	+
	C(1)	C(4)	3.557 (9)	0.063	0.008	−	0.0389	0.3402	+
	C(2)	C(3)	3.558 (7)	0.226	−0.028	+	−0.3004	−0.4870	+
	C(5)	N(1)	3.493 (7)	−0.039	−0.126	−	0.0847	0.4201	+
	C(6)	C(8)	3.473 (9)	0.318	0.096	−	0.5709	0.1753	+
	N(6)	C(7)	3.486 (11)	−0.213	−0.041	−	0.2700	−0.2933	−
	N(6)	C(8)	3.562 (8)	−0.213	0.096	+	0.2700	0.1753	+
stack IV	N(1)	C(5)	3.555 (10)	−0.063	−0.012	−	0.4040	−0.1078	−
	C(2)	C(4)	3.577 (9)	0.226	0.008	−	−0.3117	−0.3402	+
	C(2)	C(9)	3.526 (8)	0.226	−0.013	+	−0.3117	−0.0908	+
	N(3)	C(8)	3.573 (8)	−0.165	0.096	+	−0.0694	−0.1753	+
	N(3)	C(9)	3.536 (7)	−0.165	−0.013	−	−0.0694	−0.0908	+
	C(4)	C(8)	3.527 (9)	0.217	0.096	−	0.4869	−0.1753	−
	C(5)	C(7)	3.568 (11)	−0.039	−0.041	−	0.0948	0.2933	+
	C(6)	C(6)	3.580 (11)	0.318	0.014	−	0.5625	0.3012	+
	N(9)	N(1)	3.598 (7)	−0.060	−0.126	−	−0.2029	−0.4201	+

[a] Electronic energy (kcal/mol) was computed by $332.0\Sigma_i\Sigma_j q_i q_j / r_{ij}$, where r_{ij} is the distance (Å) between atom i of 3-methylindole and j of DMA^+ and q_i is the Coulombic charge on atom i. [b] Stabilization energy was calculated by using the following equation and the total energy (E) of the respective molecule: stabilization energy = E(stacked pair) − [E(3-methylindole) + $E(DMA^+)$]. For the calculations of E(stacked pair), the dihedral angle between 3-methylindole and DMA^+ molecules was treated to be 0° for the sake of clarity. [c] Electronic attraction or repulsion is designated by (+) or (−), respectively. [d] Atomic coefficients used for the LUMO of adeninium in stacks I and IV are the ones calculated by using the coordinates of stacks II and III, respectively, and the remaining coefficients of LUMO and HOMO were obtained from DMA^+ and 3-methylindole molecules, respectively. [e] The coupling or splitting of the orbital interaction is designated by (+) or (−), respectively.

96.5, 9.8, and 5.5%, respectively. As the stacked state has no fluorescence (Mutai et al., 1975; Montenay-Garestier & Helene, 1968; Montenay-Garestier & Helene, 1971), the observed quenching indicates the existence of stacking interaction in the excited states. The fluorescence of IC3MA$^+$I$^-$ and the 3-methylindole coexisting with DMA$^+$I$^-$ was meaningly quenched compared with those of IC3A and 3-methylindole coexisting with 9-methyladenine, respectively. The result also appears to indicate the importance of the N(1)-quaternization of the adenine ring for the effective indole–adenine stacking interaction.

Although the fluorescence emission spectrum of the 3-methylindole coexisting with DMA$^+$I$^-$ suggests the stacking interaction of model I in its solution state, the hypochromism observed in its UV spectrum (Ishida & Inoue, 1981a) was not so significant as that of model II. In order to clarify the stacking mode, we measured the ^{1}H NMR spectra of a DMA$^+$–IAA$^-$ (1:1) mixture (see Figure 10). The H(2) and H(8) proton signals in DMA$^+$I$^-$ shifted upfield by ca. 0.08 and 0.14 ppm upon mixing with IAA, and the methyl groups attached to the N(1) and N(9) atoms both moved upfield by ca. 0.1 ppm. The upfield shift (ca. 0.07 ppm average) of the indole ring protons of IAA, along with the ca. 0.06 ppm upfield shift of its methylene protons, was also observed in the 1:1 mixed solution. The changes in the chemical shifts are explicable by ring-current effects, because the π–π stacking

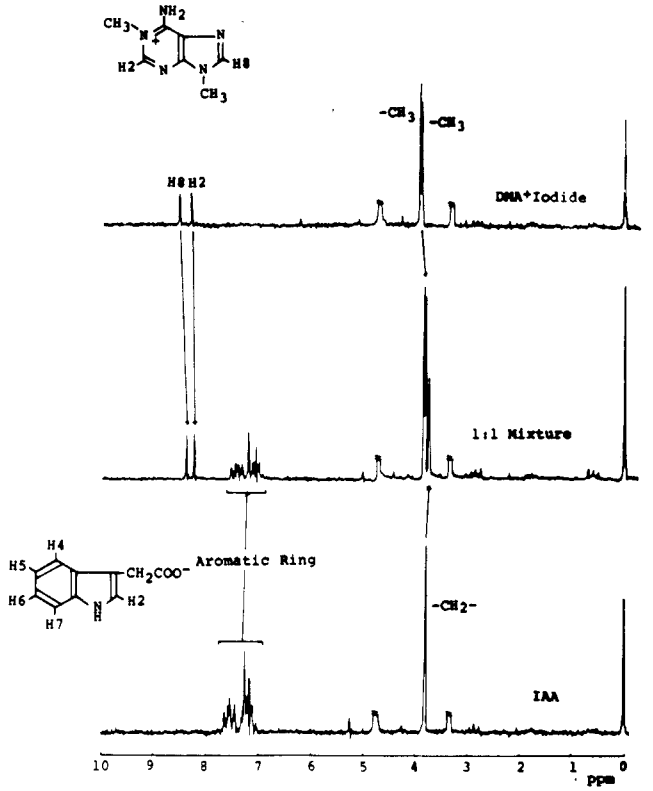

FIGURE 10: ^{1}H NMR spectra of DMA^+I^-, IAA, and their 1:1 mixture. The chemical shift was adjusted by reference to DSS as an internal standard.

interaction can cause the upfield shifts for the protons on the indole and adeninium rings. The upfield shifts of the methyl protons bounded to the N(1) and N(9) atoms of the adeninium ring and the methylene protons of the IAA side chain suggest that the indole ring may stack over the whole of adeninium ring. Such a stacking mode is rather different from that in the crystal structure (see Figure 6), in which the indole ring is located on the pyrimidine portion of the adeninium ring.

Biological Implication of Adeninium–Indole Stacking Interaction. Many eukaryotic viral and cellular RNAs have the methylated structures at the sugar or bases, which are important for biological functions of these nucleic acids such as specific recognition to the genetic code [for examples, see Shatkin (1976), Both et al. (1975), and Weber et al. (1977)]. The N(1)-alkylated purines such as 1-methyladenosine have been found in natural some tRNAs and play an important role in determining their tertiary structures [for examples, see McCloskey & Nishimura (1977), Rich (1977), and Sprinzl & Gauss (1982)]. The present X-ray crystallographic and spectroscopic studies showed that the indole ring can preferentially associate with the adeninium ring by $\pi-\pi$ stacking interaction in both the crystal and solution states. Therefore, it is reasonably presumed that the tryptophanyl residue in protein–nucleic acid recognition plays a significant role by specific $\pi-\pi$ stacking (partly charge-transfer) interaction between the indole ring and the methylated or protonated adenine base.

When the tryptophanyl residue interacts with the adeninium base of a nucleic acid, two association steps can be considered: (1) selective recognition and (2) energetically stable binding of the adeninium ring. Model I provides the information as to the former step and model II as to the latter one. The $\pi-\pi$ charge-transfer interaction is an important factor for the selective recognition of tryptophanyl residues to the adeninium base. In addition, the stacking interaction that is stabilized by dipole–dipole and HOMO–LUMO orbital couplings between both the aromatic rings is essential for the energetically stable association of both the molecules.

Acknowledgments

We are grateful to Dr. Y. Sugiura, Pharmaceutical Sciences, Kyoto University, for helpful discussion.

Supplementary Material Available

Observed and calculated structure factors, anisotropic temperature factors of non-hydrogen atoms, and coordinates and isotropic temperature factors of hydrogen atoms (31 pages). Ordering information is given on any current masthead page.

Registry No. I, 85894-28-6; II, 85894-29-7.

References

Ash, R. P., Herriott, J. R., & Deranleau, D. A. (1977) *J. Am. Chem. Soc. 99*, 4471.

Both, G. W., Banerjee, A. K., & Shatkin, A. J. (1975) *Proc. Natl. Acad. Sci. U.S.A. 72*, 1189.

Bugg, C. E., Thomas, J. M., Sundaralingam, M., & Rao, S. T. (1971) *Biopolymers 10*, 175.

Bunick, G., & Voet, D. (1982) *Acta Crystallogr., Sect. B B38*, 575.

Carter, C. W., & Kraut, J. (1974) *Proc. Natl. Acad. Sci. U.S.A. 71*, 283.

Chiang, C. C., Epps, L. A., Marzilli, L. G., & Kistenmacher, T. J. (1979) *Acta Crystallogr., Sect. B B35*, 2237.

Church, G. M., Sussman, J. L., & Kim, S. H. (1977) *Proc. Natl. Acad. Sci. U.S.A. 74*, 1458.

Cromer, D. T., & Waber, J. T. (1974) in *International Tables for X-ray Crystallography* (Ibers, J. A., & Hamilton, W. C., Eds.) Vol. IV, pp 71–73, Kynoch Press, Birmingham, England.

Dimicoli, J. L., & Helene, C. (1973) *J. Am. Chem. Soc. 95*, 1036.

Gabbay, E. J., Adawadkar, P. D., Kapicak, L., Pearce, S., & Wilson, W. D. (1976) *Biochemistry 15*, 152.

Helene, C., & Maurizot, J. C. (1981) *CRC Crit. Rev. Biochem. 10*, 213.

Helene, C., & Lancelot, G. (1982) *Prog. Biophys. Mol. Biol. 39*, 1.

Helene, C., Dimicoli, J. L., & Brun, F. (1971) *Biochemistry 10*, 3802.

Helene, C., Brun, F., Charlier, M., & Yaniv, M. (1976) *Biochem. Biophys. Res. Commun. 71*, 91.

Herriott, J. R., Camerman, A., & Deranleau, D. A. (1974) *J. Am. Chem. Soc. 96*, 1585.

Inoue, M., Sakaki, T., Fujiwara, T., & Tomita, K. (1978) *Bull. Chem. Soc. Jpn. 51*, 1118.

Ishida, T. (1979) Dissertation, Faculty of Pharmaceutical Sciences, p 109, Osaka University, Osaka, Japan.

Ishida, T., & Inoue, M. (1981a) *Biochem. Biophys. Res. Commun. 99*, 149.

Ishida, T., & Inoue, M. (1981b) *Acta Crystallogr., Sect. B B37*, 2117.

Ishida, T., Inoue, M., Senda, S., & Tomita, K. (1979) *Bull. Chem. Soc. Jpn. 52*, 2953.

Ishida, T., Usami, H., Inoue, M., Yamagata, Y., & Tomita, K. (1982) *Biochem. Biophys. Res. Commun. 107*, 746.

Jallon, J. M., Risler, Y., Schneider, C., & Thiery, J. M. (1973) *FEBS Lett. 31*, 251.

Jones, J. W., & Robins, R. K. (1963) *J. Am. Chem. Soc. 85*, 193.

Kaneda, T., & Tanaka, J. (1976) *Bull. Chem. Soc. Jpn. 49*, 1799.

Karle, I. L., Britts, K.,& Gum, P. (1964) *Acta Crystallogr. 17*, 496.
Karle, I. L., Dragonette, K. S., & Brenner, S. A. (1965) *Acta Crystallogr. 19*, 713.
Kolodny, N. H., & Neville, A. C. (1980) *Biopolymers 19*, 2223.
Kolodny, N. H., Neville, A. C., Coleman, D. L., & Zamecnik, P. C. (1977) *Biopolymers 16*, 259.
Lawaczeck, R., & Wagner, K. G. (1974) *Biopolymers 13*, 2003.
Lefevre, J. F., Ehrlich, R., Kilhoffer, M. C., & Remy, P. (1980) *FEBS Lett. 114*, 219.
Main, P., Hull, S. E., Lessinger, L., Germain, G., Declercq, J. P., & Woolfson, M. M. (1978) *MULTAN 78. A System of Computer Programs for the Automatic Solution of Crystal Structures from X-Ray Diffraction Data*, University of York, England, and Louvain, Belgium.
McCloskey, J. A., & Nishimura, S. (1977) *Acc. Chem. Res. 10*, 403.
Montenay-Garestier, T., & Helene, C. (1968) *Nature (London) 217*, 844.
Montenay-Garestier, T., & Helene, C. (1971) *Biochemistry 10*, 300.
Mutai, K., Gruber, B. A., & Leonard, N. J. (1975) *J. Am. Chem. Soc. 97*, 4095.
Ohki, M., Takenaka, A., Shimanouchi, H., & Sasada, Y. (1977a) *Bull. Chem. Soc. Jpn. 50*, 2573.
Ohki, M., Takenaka, A., Shimanouchi, H., & Sasada, Y. (1977b) *Acta Crystallogr., Sect. B B33*, 2954.
Ondik, H., & Smith, D. (1968) in *International Tables for X-ray Crystallography* (Macgillavry, C. H., Rieck, G. D., & Lonsdale, K., Eds.) Vol. III, p 273, Kynoch Press, Birmingham, England.
Pople, J. A., & Segal, G. A. (1966) *J. Chem. Phys. 44*, 3289.
Pullman, B., & Pullman, A. (1958) *Proc. Natl. Acad. Sci. U.S.A. 44*, 1197.
Rich, A. (1977) *Acc. Chem. Res. 10*, 388.
Sakaki, T., Sogo, A., Wakahara, A., Kanai, T., Fujiwara, T., & Tomita, K. (1976) *Acta Crystallogr., Sect. B B32*, 3235.
Shatkin, A. J. (1976) *Cell (Cambridge, Mass.) 9*, 645.
Slifkin, M. A. (1971) in *Charge Transfer Interactions of Biomolecules*, Academic Press, London and New York.
Sprinzl, M., & Gauss, D. H. (1982) *Nucleic Acids Res. 10*, 1.
Steitz, T. A., Ohlendorf, D. H., McKay, D. B., Anderson, W. F., & Mattews, B. W. (1982) *Proc. Natl. Acad. Sci. U.S.A. 79*, 3097.
Tavale, S. S., Sakore, T. D., & Sobell, H. M. (1969) *J. Mol. Biol. 43*, 375.
Taylor, R., & Kennard, O. (1982a) *J. Am. Chem. Soc. 104*, 3209.
Taylor, R., & Kennard, O. (1982b) *J. Mol. Struct. 78*, 1.
Toulme, J. J., & Helene, C. (1980) *Biochim. Biophys. Acta 606*, 95.
UNICS (1979) The Universal Crystallographic Computing System–Osaka, The Computation Center, Osaka University.
Vasak, M., Nagayama K., Wüthrich, K., Mertens, M. L., & Kägi, J. H. R. (1979) *Biochemistry 18*, 5050.
Wagner, K. G., & Lawaczeck, R. (1972) *J. Magn. Reson. 8*, 164.
Warrant, R. W., & Kim, S. H. (1978) *Nature (London) 271*, 130.
Weber, L. A., Hickey, E. D., Nuss, D. L., & Baglioni, C. (1977) *Proc. Natl. Acad. Sci. U.S.A. 74*, 3254.
Yamauchi, K., Tanabe, T., & Kinoshita, M. (1976) *J. Org. Chem. 41*, 3691.
Yoshino, H., Morita, F., & Yagi, K. (1972) *J. Biochem. (Tokyo) 72*, 1227.

Site-Directed Mutagenesis as a Probe of Enzyme Structure and Catalysis: Tyrosyl-tRNA Synthetase Cysteine-35 to Glycine-35 Mutation†

Anthony J. Wilkinson, Alan R. Fersht,* David M. Blow, and Greg Winter*

ABSTRACT: Oligodeoxynucleotide-directed mutagenesis has been used on the gene of tyrosyl-tRNA synthetase from *Bacillus stearothermophilus* to produce mutant enzymes altered at the adenosine 5′-triphosphate (ATP) binding site. Deliberate attempts were made to alter rather than destroy enzymic activity so that kinetic measurements may be made to identify the subtle roles of the enzyme–substrate interactions in catalysis. Cys-35, the -SH group of which is involved in binding the 3′-OH of the ribose ring of ATP, has been mutated to a serine residue [Winter, G., Fersht, A. R., Wilkinson, A. J., Zoller, M., & Smith, M. (1982) *Nature (London) 299*, 756–758] or glycine residue. The mutant enzymes are less active than the wild type, and the reduction in activity can be attributed to a decrease in the value of k_{cat} and an increase in K_M. Thus, the interaction energy of the side chain of Cys-35 with the substrate is not fully realized in the enzyme–substrate complex but is used preferentially to stabilize the transition state. Relative to its absence in the Gly-35 mutant, the side chain of Cys-35 is calculated to stabilize the transition state for pyrophosphate exchange by 1.2 kcal/mol and the transition state for aminoacylation by 1.0 kcal/mol.

It is now possible to alter any amino acid residue of a protein at will by site-directed mutagenesis of its gene. The rapid advances in solid-phase synthesis of oligodeoxynucleotides and the introduction of the technique of oligodeoxynucleotide-directed mutagenesis (Hutchinson et al., 1978) have facilitated the construction of point mutations in DNA [see Itakura (1982) and Smith (1982) for brief reviews]. The application of this technique to the tyrosyl-tRNA synthetase from *Bacillus stearothermophilus* has previously been described (Winter et al., 1982). In outline (see Figure 1), the gene coding for the enzyme was cloned into the bacteriophage vector M13; a short

† From the Departments of Chemistry (A.J.W. and A.R.F.) and Physics (D.M.B.), Imperial College of Science and Technology, London SW7 2AY, U.K., and the MRC Laboratory of Molecular Biology (G.W.), Cambridge CB2 2QH, U.K. *Received February 4, 1983.* This work was supported by the MRC of the U.K.

0006-2960/83/0422-3581$01.50/0